Interaction of Ag, Rh, and Pd Atoms with MgO Thin Films Studied by the CO Probe Molecule

Ken Judai, Stéphane Abbet, Anke S. Wörz, and Ulrich Heiz*

Institute of Surface Chemistry and Catalysis, University of Ulm, Albert-Einstein-Allee 47, D-89069 Ulm, Germany

Livia Giordano and Gianfranco Pacchioni

Dipartimento di Scienza dei Materiali, Università Milano-Bicocca and Istituto Nazionale per la Fisica della Materia, via R. Cozzi 53, I-20125 Milano, Italy

Received: February 7, 2003; In Final Form: June 2, 2003

The interaction of carbon monoxide with Ag, Rh, and Pd atoms deposited on MgO thin films has been studied by thermal desorption and Fourier transform infrared spectroscopies. To obtain an atomistic view of the surface complexes, we performed density functional calculations on cluster models of the MgO(100) surface. The combined experimental−theoretical information leads to the following picture. Ag atoms interact weakly with the surface and do not form stable complexes with CO. Pd atoms become trapped at oxygen vacancies (F centers) already at low temperature; at these sites $Pd(CO)_2$ complexes form after exposure to CO. The CO molecules desorb from these sites at $T = 230$ K. At higher temperature, 370 K, we observe formation of small Pd aggregates with bridge-bonded CO molecules, indicating diffusion of Pd atoms or Pd(CO) units. Rh atoms bind quite strongly to the oxide anions at steps where they form relatively stable $Rh(CO)_2$ or even $Rh(CO)_3$ complexes; a minority of the Rh atoms populates the F centers. A first CO desorption occurs at 180 K and leaves on the surface rather mobile, very stable Rh(CO) units which diffuse until they become trapped at F centers; at 390 K a second CO desorption occurs leaving on the surface isolated Rh atoms, with no indication of formation of small Rh aggregates.

1. Introduction

Deposition of metal atoms and clusters on the surface of oxide materials is a topic attracting increasing interest because of several technological applications of metal−oxide interfaces.[1−4] In recent years, very accurate experiments have been designed in order to get deeper insight into the mechanism of the interaction of metal nanoaggregates on oxide surfaces.[1,2,5] These techniques make use of thin oxide films grown in ultrahigh-vacuum conditions on a conducting substrate to simulate the morphology and the electronic structure of oxide materials. In this way the problems connected to the insulating and brittle nature of the ceramic oxides are removed. Metal deposition has been done mainly by vaporizing the metal on the substrate kept at very low temperature. By careful control of the deposition conditions, it has been possible to grow small and rather well-defined nanoparticles and, in a few cases, even to stabilize isolated metal atoms on the surface. An alternative technique, developed in our group, is to generate the metal atoms or clusters in a cluster source so that the aggregates can be selected by mass before deposition onto the surface. The use of soft-landing techniques, deposition at low temperature and low concentration, prevents the agglomeration of the deposited metals.[6,7] As a result, we obtain mass-selected, monodispersed clusters on a substrate.

There is general consensus that one of the most critical aspects of these techniques is connected to the rich and complex nature of the oxide substrate and, in particular, to the role that point or extended defects have in the stabilization of the deposited species and even in their chemical modification. In this respect, a detailed mapping of the surface sites is crucial, as it has been shown that even a simple surface like MgO can expose adsorption sites with very different characteristics. This is important, not only in determining the initial sites where the metal atoms or clusters are stabilized when they land on the surface but also in identifying the mechanisms of diffusion as the temperature is increased. Adsorption of CO on deposited metal atoms or clusters provides very useful, although indirect, information about the metal adsorption site, the chemical modification due to the metal−oxide interface bonding, and the evolution of the properties as a function of the temperature.[8] However, the simple analysis of experimental evidence is not sufficient to formulate a well-grounded hypothesis about the microscopic structure of the adsorption sites. An atomistic view of the system can be obtained by combining experiments with first principles calculations.[9−11]

In this work we present a combined experimental−theoretical study of the deposition of Ag, Pd, and Rh atoms on MgO thin films and of their interaction with CO molecules. Thermal desorption spectroscopy (TDS) is used to determine the strength of the bond of the CO molecules to the deposited metal atoms; this is essential information for identifying the metal adsorption site. Fourier transform infrared (FTIR) spectroscopy is used to follow the changes in C−O stretching frequency as a function of metal, temperature, and adsorption site, etc. The experimental observations are complemented by first principles density functional theory (DFT) calculations on metal−carbonyl complexes deposited on various sites of the MgO surface represented by embedded cluster models. From a careful analysis of

10.1021/jp034324w CCC: $25.00
Published on Web 08/05/2003

experimental and theoretical results, we propose an explanation of the observed behaviors, which, not surprisingly, are rather different for the three metals considered.

The paper is organized as follows. In Section 2 we give the essential details of the experiments and of the computations. Section 3 reports the experimental and the computational results. Section 4 combines the various observations and provides a tentative explanation of the measurements. Section 5 summarizes our conclusions.

2. Experimental and Computational Details

2.1. Experiments. Metal clusters of Ag, Pd, and Rh are produced by a recently developed high-frequency laser evaporation source.[5] The positively charged cluster ions are guided by home-built ion optics through differentially pumped vacuum chambers and are size-selected by a quadrupole mass spectrometer (Extranuclear C50/mass limit: 9000 amu). The silver, palladium, and rhodium atoms are then deposited with low kinetic energy ($E_{kin} < 2$ eV/atom) onto magnesium oxide thin films of ~10 monolayers thickness, as estimated by Auger electron spectroscopy. Upon impact the atomic ions are neutralized either on defect sites (F centers) or by charge tunneling through the thin MgO films. We deposited 0.8 and 2.0% monolayer of metal atoms (1 monolayer $= 2.25 \times 10^{15}$ atoms/cm^2) at 90 K for the TDS and infrared experiments, respectively, to land them on an isolated area of the surface and to prevent agglomeration. In fact, recent Monte Carlo simulations showed that at these low coverages at least 92% of the atoms are landing isolated on the surface.[6] The MgO(100) films are prepared in situ for each experiment; they are epitaxially grown on a Mo(100) surface by evaporating magnesium in a $^{16}O_2$ background and subsequently annealing the sample to 1000 K.[12] These films show bulklike structural and electronic properties as observed by low electron energy diffraction (LEED), X-ray photoelectron spectroscopy (XPS), UV photoelectron spectroscopy (UPS), and electron energy loss spectroscopy (EELS).[13] However, extended defects such as steps and kinks as well as point defects are detected by scanning tunneling microscopy.[5]

For the thermal desorption experiments the samples are dosed at 90 K, using a calibrated molecular beam doser, to about 0.1 langmuir of ^{13}CO, resulting in saturation coverage on the deposited atoms as physisorbed CO from the MgO surface is observed. Saturation coverage occurs via reverse spillover of CO from the oxide surface to the cluster upon heating. In thermal desorption experiments the sample is heated with a rate of 2 K/s and the desorbing molecules are detected by a mass spectrometer (Balzers QMG 421). The reproducibility of the experiments lies within 7%, and thus the obtained spectra can be compared quantitatively. For these experiments we used minimal exposures to suppress the large contribution of CO desorbing from the oxide surface. For the infrared experiments the samples were exposed to 3 langmuirs of ^{13}CO. At these higher exposures the clusters are saturated already at 90 K via direct adsorption. As in these experiments we selectively detect the CO molecules; on different adsorpion sites we can use higher exposures. The FTIR measurements were performed in single reflection mode. All the spectra are taken at 95 K after a flash to the indicated temperature. A set of 512 interferograms is averaged, and no smoothing was carried out; the resolution was set to 4 cm^{-1}.

2.2. Computations. The interaction of CO with Ag, Pd, and Rh atoms adsorbed on regular and low-coordinated O sites or F centers of the MgO surface has been studied with embedded cluster models.[14] The binding energy and the vibrations of CO molecules adsorbed on the three metal atoms have been obtained with gradient corrected density functional theory (DFT). We used the hybrid Becke3 functional for exchange[15] and the Lee−Yang−Parr functional for correlation,[16] B3LYP. We used a large set of +2 and −2 point charges (PC) placed at the lattice positions to reproduce the Madelung potential inside the cluster. The occurrence of an artificial polarization of the oxide anions at the cluster border has been avoided by placing an effective core potential (ECP) on the positive charges around the quantum-mechanical cluster.[17] This approach has been widely tested versus more elaborated embedding schemes or periodic calculations. A test case has been that of CO on MgO for which all possible theoretical methods have been applied, showing the adequacy of the cluster approach.[18]

The MgO sites have been modeled by the following clusters: $O_{13}Mg_{13}$ represents a five-coordinated O_{5c} ion at a terrace or, by removing one O atom, the corresponding F_{5c-} or F_{5c}^+ centers; bridge sites over two adjacent oxide anions on the MgO terraces have been simulated by Mg_8O_{14} clusters: $O_{12}Mg_{10}$ models a binding site involving an O_{5c} and a four-coordinated O_{4c} ion at a step site. The convergence of the results versus the size of the cluster has been checked in a previous work for the case of Pd;[8] oscillations of about 5% are expected on the metal binding energies, while the CO properties show smaller oscillations, ±0.1 eV for the adsorption energy and ±10 cm^{-1} for the frequencies.

Gaussian-type atomic orbital basis sets were used to construct the Kohn−Sham orbitals. The basis set used for the Mg and O ions of the substrate cluster is the 6-31G;[19] when an O atom is removed to form an F center, one has to adopt a sufficiently flexible basis set to describe the electron localization in the vacancy. This can be achieved by adding floating functions at the cavity center[20] or by using a more diffuse basis set on the neighboring Mg ions.[20] Here, we adopted this second strategy and we used for the Mg ions around the vacancy a 6-31+G-(2p,2d) basis set. The Ag, Pd, and Rh atoms were treated by an 18-electrons ECP, which includes in the valence the $4s^24p^64d^n5s^m$ electrons; the basis set is of double-ζ plus polarization type.[21] For CO we used a 6-311G* basis (test calculations show that the use of the larger 6-311+G(2d,2p) basis for CO does not change the properties in a significant way). The binding energies, E_b, of the metal atoms to MgO have been corrected for the basis set superposition error (BSSE).[22] No correction has been applied to the CO binding energies, and all the corresponding E_b values are somewhat overestimated because of this effect; this error has been estimated in a previous paper for the case of Pd, and it amounts to 0.2−0.3 eV.[8]

The geometries of CO, of the metal atom, and of the first neighbors on the MgO surface have been fully optimized by means of analytical gradients. A full vibrational analysis, based on second derivatives of the total energy, has been performed to compute the harmonic frequency of CO, ω_0. For the cases where CO is normal to the surface, ω_0(CO) has been determined by fitting the potential energy curve by a fifth-degree polynomial. With the 6-311G* basis set the CO ω_0 computed at the B3LYP level is 2221 cm^{-1}, while the experimental harmonic frequency is 2170 cm^{-1} (the experimental anharmonic value is $\omega_e = 2143$ cm^{-1}).[23] Therefore, all the frequencies have been scaled by a factor of 2170/2221 = 0.977 in order to take into account the overestimate of the free CO ω_0. In this way the computed C−O frequencies for gas-phase metal−carbonyl complexes are in close agreement with experiment, Table 1. However, we found that the computed frequencies for the MgO-

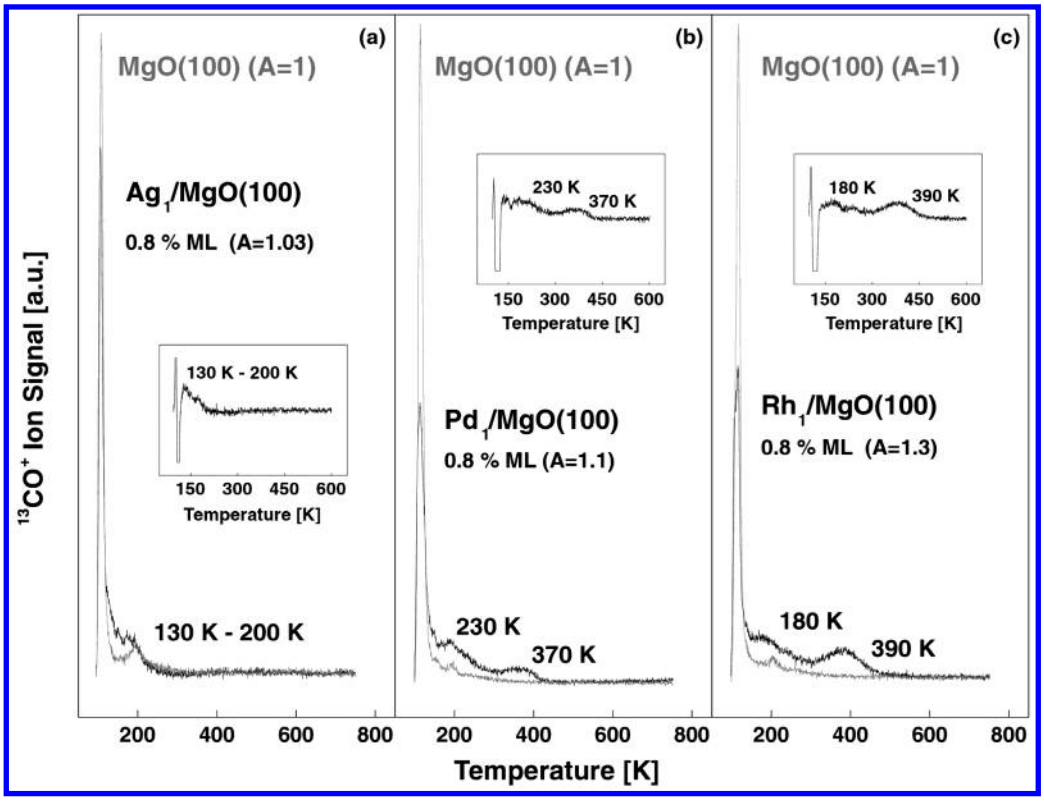

Figure 1. CO desorption spectra taken before and after the deposition of Ag (a), Pd (b), and Rh atoms (c) onto thin MgO(100) films. For all three samples, 0.8% monolayer atoms were deposited at 90 K and the sample were exposed to the identical number of CO molecules per atom (see text). Note the different number of desorbing CO molecules from the three samples calculated from the area of the TDS spectra (*A*). The insets show the difference spectra of the sample prior to and after atom deposition.

TABLE 1: Computed and Measured Vibrational Frequencies (cm^{-1}) for Free ^{12}CO and ^{12}CO Adsorbed on Rh, Rh^+, Pd, and Pd^+

	ω_0(calc)	ω_0(scaled)[a]	expt
CO	2221	2170	2143 (ω_e), 2170 (ω_0)
Rh(CO)	2055	2008	2008-2023
$Rh(CO)_2$	2082, 2170	2034, 2121	
$[Rh(CO)]^+$	2262	2210	2174
Pd(CO)	2121	2072	2056
$[Pd(CO)]^+$	2289	2236	2206

[a] A scaling factor 0.977 has been applied.

supported species are systematically too low compared to the experimental values. One reason is that our MgO clusters are embedded in a PC field, which reduces the C−O ω_0 by 30−50 cm^{-1} (it has been suggested that bare MgO clusters are indeed better for the calculation of vibrations of adsorbed molecules).[24] A second reason is that it is possible that charge-transfer effects from the surface oxide anions to the adsorbed metal, and the consequent back-donation to CO, are overestimated in our models. Finally, one should not forget that the frequencies are computed in the harmonic approximation and that anharmonic effects are not included.

All the calculations have been performed with the GAUSSIAN98[25] program package.

3. Results

3.1. Experiments. Figure 1 shows the TDS of ^{13}CO for the three metal atoms (Ag, Pd, and Rh) deposited on thin MgO(100) films. As comparison, the ^{13}CO-desorption spectra (in gray) are also shown for the clean thin films. These spectra were taken just before the corresponding metal atoms were deposited on the surface. For the MgO films it is well-known that the CO-desorption at low temperature (below 200 K) originates from CO adsorbed on low-coordinated cation sites.[18] In the case of silver atoms a small contribution to the CO-desorption after metal deposition is observed in the temperature range of 130−200 K (Figure 1a). This Ag-specific desorption is even better illustrated when taking the difference of the two TDS spectra (see inset of Figure 1a). The corresponding binding energy is estimated to be between 0.3 and 0.5 eV when using the Redhead approximation. The CO-desorption from Pd atoms is more pronounced and reveals two desorption peaks around 230 (0.6 eV) and 370 K (1.0 eV), respectively. The precise position of the low-temperature desorption is difficult to extract because it overlaps with the small contribution of the clean MgO(100) film. The difference spectrum is shown in the inset of Figure 1b. The integral of the low-temperature peak (230 K) is slightly larger than the one of the high-temperature peak. Note the distinct decrease of the 120 K desorption originating from CO adsorbed to the thin MgO(100) film. Since the CO dosage is well below saturation of the low-coordinated cation sites of the substrate and constant for both experiments, this decrease can be attributed to a change in the occupation from the substrate to high-energy binding sites introduced by the presence of the Pd atoms. Note also that the integral of the two spectra shown in Figure 1b is close to constant. The CO-desorption from deposited Rh-atoms is very similar and reveals two desorption peaks at 180 (0.5 eV) and 390 K (1.1 eV) (Figure 1c); the occupation of the high-energy binding sites is, however, significantly higher, and the total integral of the desorbing CO from Rh/MgO(100) increased by a factor of 1.3. This indicates that the CO-sticking coefficient has increased; thus, in contrast to the Pd case, the high binding energy site has to be present already at low temperature.

These results show distinct differences in the interaction of CO with the three metal atoms. CO hardly interacts with

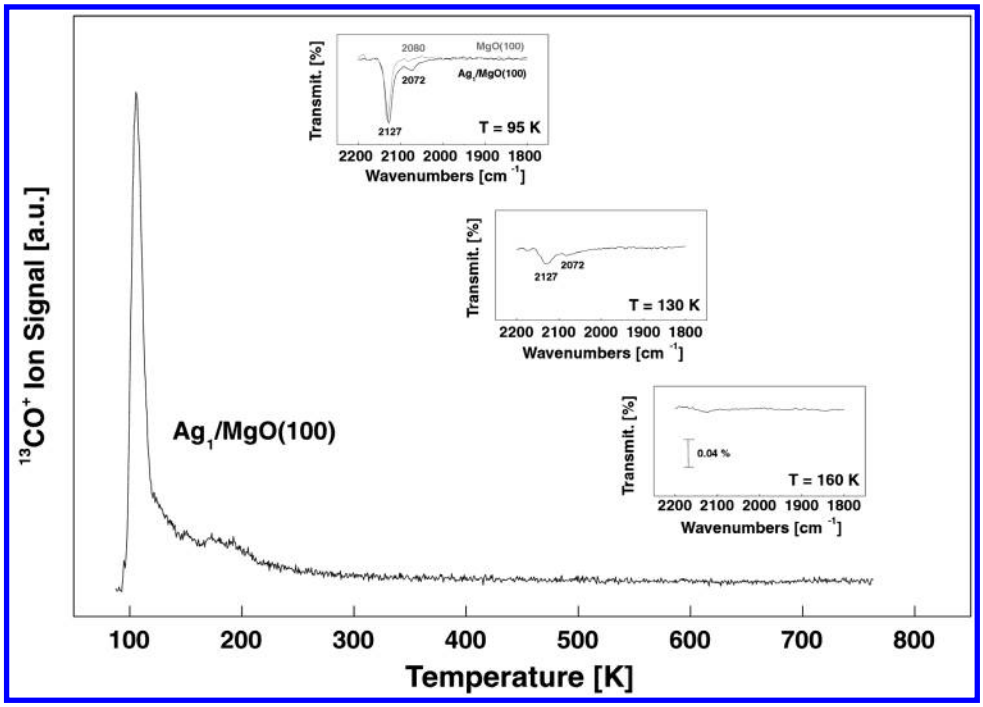

Figure 2. TPD spectrum of CO from a $Ag_1/Mg(100)$ sample. The insets show the evolution of the measured CO frequency with temperature. At 95 K the FTIR spectrum is also shown for a clean CO-covered MgO(100) thin film.

deposited Ag atoms ($E_b = 0.3-0.5$ eV). For the other two atoms the CO interaction is stronger (E_b(Pd) = 0.6 and 1.0 eV; E_b(Rh) = 0.5 and 1.1 eV). The origin of the two desorption peaks, however, cannot be obtained from these data alone. Possible origins are as follows: (i) desorption of differently bonded CO molecules from a single metal atom, (ii) desorption of CO molecules bonded from metal atoms adsorbed on various sites, and (iii) desorption of CO molecules from metastable atoms/clusters (larger clusters can be formed on the surface upon heating during the TDS experiment).

To disentangle these different origins, infrared spectroscopy can provide valuable information; one should keep in mind, however, the selection rule that only vibrations with components of the dynamical dipole perpendicular to the surface can be measured. Figure 2 shows infrared spectra of the Ag_1/MgO(100) sample after exposure of ^{13}CO and annealing to the indicated temperature; comparison of the TDS of CO is also depicted in this figure. At 95 K, two adsorption bands are observed at 2127 and 2072 cm^{-1}. A comparison with the infrared spectrum of the clean MgO(100) suggests that both bands (2127 and 2080 cm^{-1}) can be attributed to CO adsorbed on low-coordinated cation sites of the MgO surface. The intensity of low-frequency band (2072 cm^{-1}) is, however, slightly enhanced for the Ag_1/MgO(100) sample and shifted by 8 cm^{-1} to the red, suggesting that part of this band can be attributed to new adsorption sites formed after Ag deposition. This assignment is supported by its temperature evolution (it disappears at temperatures below 160 K), which is consistent with the TDS results (CO-desorption from Ag_1/MgO(100) below 190 K).

The infrared spectra of CO on Pd atoms (Figure 3) are more complex and the origin of the observed peaks has already been discussed in an earlier publication.[8] It was found that the band at 2045 cm^{-1} with the shoulder at 2010 cm^{-1} can be assigned to two CO molecules bound on a single Pd atom adsorbed on an oxygen vacancy (F- or F^+ center);[8] this indicates that the Pd atom is trapped to an oxygen vacancy already at low temperature during or after the deposition. Upon heating to about 180 K one CO molecule is desorbing (hidden in the large contribution of CO-desorption from the MgO(100) in the TDS) and the band at 2010 cm^{-1} is attributed to a single CO molecule bound to the Pd atom trapped on the oxygen vacancy. Note, that the Pd-atom on this defect site is stable up to 250 K as the infrared spectrum is reversible after annealing to this temperature and redosing CO (inset of Figure 3). Upon annealing to higher temperatures a band at 1830 cm^{-1} appears around 300 K just before the observation of the second desorption peak in the TDS. This frequency can only be explained if we consider a bridge-bonded CO on palladium. Thus, at higher temperatures Pd atoms migrate on the surface and form larger clusters. In fact, ab initio calculations revealed a vibrational frequency of CO bound in a bridge configuration to deposited Pd_2 of 1830 cm^{-1}.[26] The band at 1830 cm^{-1} disappears at the same temperatures (~400 K) as CO desorption is observed by TDS (Figure 3).

The TD and infrared spectra of CO adsorbed on deposited Rh atoms are depicted in Figure 4. Considering the similarities of the TD spectra for Rh and Pd atoms, we may expect the same mechanism for Rh atoms to occur as for Pd atoms. This is, however, not consistent with the infrared data; the formation of larger Rh particles can be unambiguously excluded by the absence of vibrational frequencies typical for higher coordinated CO (~1830 cm^{-1}; bridge-bonded ^{13}CO).[27] A closer look at the evolution of the infrared spectra with temperature suggests the following mechanism. At 95 K two bands at 2040 and 2010 cm^{-1} are observed, indicating that at least two differently bonded CO molecules exist on the deposited Rh atoms. Annealing the sample to temperatures of about 300 K results in a single band at 2000 cm^{-1}. This observation is consistent with the desorption of CO at around 180 K observed by TDS. Interestingly, redosing the system with CO after annealing the sample to 230 K results in an identical spectrum as observed at 95 K (inset Figure 4). This observation leads to the conclusion that the Rh atom is stable at least up to this temperature. The corresponding adsorption site of Rh on the MgO(100) surface is labeled by A. Annealing the sample to temperatures higher than 300 K leads to an nonreversible change after redosing CO (inset Figure

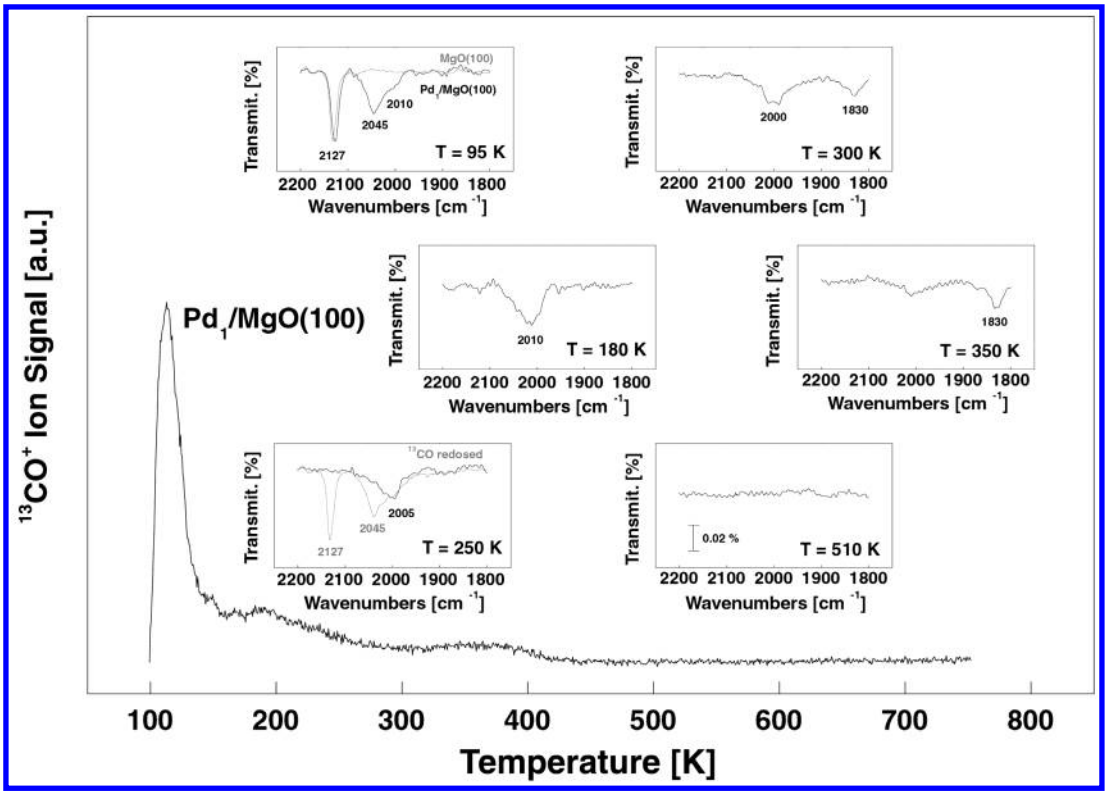

Figure 3. TPD spectrum of CO from a $Pd_1/Mg(100)$ sample. The insets show the evolution of the measured CO frequency with temperature. At 95 K the FTIR spectrum is also shown for a clean CO-covered MgO(100) thin film. At 250 K the FTIR results also show a spectrum obtained after annealing the sample to this temperature and redosing CO.

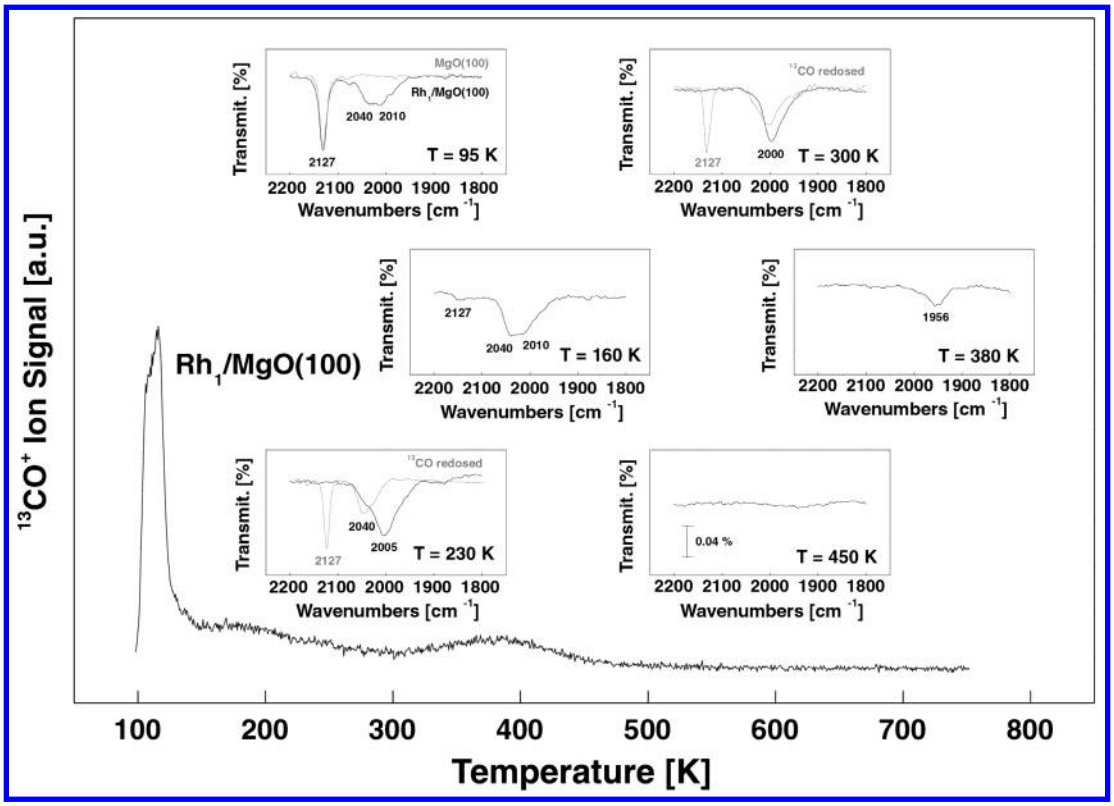

Figure 4. TPD spectrum of CO from a $Rh_1/Mg(100)$ sample. The insets show the evolution of the measured CO frequency with temperature. At 95 K the FTIR spectrum is also shown for a clean CO-covered MgO(100) thin film. At 230 and 300 K the FTIR results also show spectra obtained after annealing the sample to these temperatures and redosing CO.

4); the resulting infrared spectrum reveals only a single absorption band at 2000 cm^{-1}. This change can be explained if we allow the Rh atom to migrate to a second adsorption site B without forming larger clusters. If the sample is annealed to even higher temperatures, the absorption band shifts to 1956 cm^{-1} and disappears at around 450 K, exactly in the temperature range where the second CO-desorption is observed by TDS. The identification of the two adsorption sites cannot be done

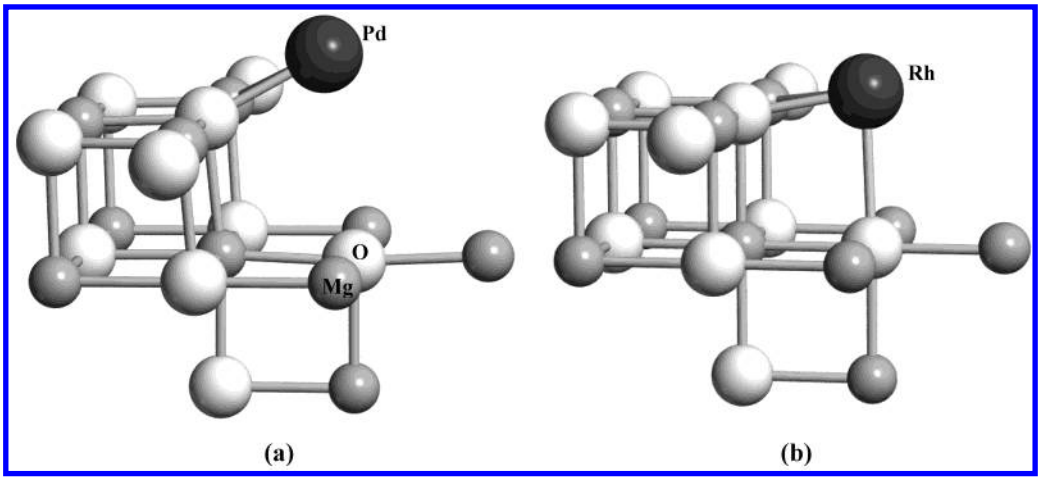

Figure 5. Optimal geometries of Pd (a) and Rh (b) metal atoms adsorbed at a step on the MgO surface.

TABLE 2: Adsorption Energies of Ag, Pd, and Rh Atoms on MgO Terraces and Steps and Surface F_{5c} and F_{5c}^+ Centers[a]

	O_{5c}(terrace)	O_{4c}–O_{5c}(step)	F_{5c}	F_{5c}^+
Ag	$^2A_1$	^2A	$^2A_1$	$^1A_1$
E_b(Ag), eV	0.48	0.67	1.54	2.02
Pd	$^1A_1$	^1A	$^1A_1$	$^2A_1$
E_b(Pd), eV	0.96	1.41	3.42	2.10
Rh	$^2B_2$	^2A	$^2B_2$	$^3B_1$
E_b(Rh), eV	0.97	1.95	3.21	2.10

[a] All values have been corrected by the basis set superposition error (BSSE).

TABLE 3: Difference in Stabilities (eV) of Rh and Pd Atoms and Rh(CO) and Pd(CO) Complexes Adsorbed on Various Sites on the MgO Surface[a]

	$O_{5c} \rightarrow O_{5c}$–$O_{5c}$ (bridge)	O_{4c}–O_{5c} (step) $\rightarrow O_{5c}$	$F_{5c} \rightarrow O_{5c}$
Ag	0.24	0.19	1.06
Rh	0.12	0.98	2.24
Pd	0.41	0.45	2.46
Rh(CO)	1.01	0.92	0.83
Pd(CO)	0.73	0.40	0.84

[a] The reported values correspond to the energy cost to displace a species from one site to another one.

by these experiments alone; therefore, we compare in the following section the obtained experimental results with extensive ab initio calculations to obtain a more detailed picture of the trapping centers and the dynamics of these three different metal atoms on the MgO(100) film.

3.2. Computations. For each atom, Ag, Rh, and Pd, several adsorption sites have been considered (oxygen anions at flat terraces or steps, F- and F^+ centers located at terraces, steps, and corners). For each metal atom and for each adsorption site the formation of M(CO), $M(CO)_2$, and, for some cases, $M(CO)_3$ complexes has been studied. Sometimes more than one electronic state is involved (changes in the spin multiplicity of the transition metal atom may occur as CO molecules are added to the complex or as a result of the interaction with the adsorption site). This gives rise to a large set of data. Here, we report only the main features of the extensive calculations related to metal adsorption, CO binding energies, and C−O stretching frequencies and try to use this information to construct a coherent picture emerging from theory and experiment. We restrict the analysis to the following adsorption sites: terrace and step oxide anions; neutral and charged oxygen vacancies at terrace sites (F_{5c}- and F_{5c}^+ centers). Oxygen vacancies at low-coordinated sites have also been considered, but the general conclusions do not change. A complete and systematic report of the theoretical results, including geometrical and structural details, will be given in a separate publication.[28]

We first consider the properties of the isolated Ag, Pd, and Rh atoms deposited on the MgO surface, Table 2. On a terrace O_{5c} ion Ag is bound by 0.48 eV; slightly larger energies are found for Pd (0.96 eV) and Rh (0.97 eV). Not surprisingly, the binding becomes much stronger at defect sites, like F_{5c}- or F_{5c}^+ centers, or a step (Table 2). At F_{5c} centers Pd and Rh exhibit similarly strong adsorption energies, 3.42 and 3.21 eV, respectively; Ag is bound on F_{5c} by 1.54 eV only. The situation is quite different for step sites, Figure 5. In fact, Pd is not only less strongly bound (1.41 eV) at a step site than Rh (1.95 eV; see Table 2), but more important the adsorption geometry is different. Pd is bound with the O_{4c} site only (Figure 5a), while Rh interacts simultaneously with the O_{4c} and the O_{5c} sites (Figure 5b), acting as a bidentate ligand. This observation has important consequences for the interpretation of the results. In fact, while for Rh the step sites can act as traps where surface diffusion is blocked at low temperature, this is no longer true for Pd. The tendency of metal atoms to diffuse on the MgO surface is a key aspect in this work. The deposition is done at low temperature, 90 K, and if the barrier to diffusion is <0.3 eV, one can expect a substantial mobility even at this temperature. Since the flat (100) terraces constitute the majority of the exposed sites of the MgO films, we expect that a dominant fraction of the metal atoms will land on terraces and become stabilized at the O_{5c} anions (the binding at the cation sites is much weaker). To interpret the experimental observations, we have thus estimated the barriers for diffusion by placing a metal atom in a bridge position over two adjacent O_{5c} anions. This site is unstable, and a full geometry optimization leads to adsorption in an on-top configuration of an O_{5c} anion. In the bridge position we performed a constrained optimization of the vertical distance, without allowing lateral displacements of the adatom. The computed quantities are therefore only upper bounds to the real barriers. We found values of 0.24 eV for Ag, 0.41 eV for Pd, and 0.12 eV for Rh (Table 3). It is interesting to note that Rh exhibits very low barriers; this is connected to a general tendency of Rh to act as a bidentate ligand, at variance with Pd. These barriers are such that atom diffusion on terraces should be easy at 90 K for Rh and Ag and limited for Pd. However, one has to remember that the atoms possess some kinetic energy when they land on the surface, and the sum of the temperature effect and the residual kinetic energy could be sufficient to induce diffusion. We have also considered the energy required to displace an atom from a

TABLE 4: Properties of ^{12}CO Molecules Adsorbed on Ag, Pd, and Rh Atoms Stabilized at Various Sites of the MgO Surface[a]

	M	O_{5c} (terrace)/M	O_{4c}–O_{5c} (step)/M	F_{5c} (terrace)	F_{5c}^+ (terrace)
E_b[Ag(CO)→Ag+CO], eV	none	none	0.27	0.17	0.05
E_b[Pd(CO)→Pd+CO], eV	1.80	2.34	2.32	0.63	0.82
ω_0[Pd(CO)], cm^{-1}	2072	2029	2033	2013	2091
E_b[$Pd(CO)_2$→Pd(CO)+CO], eV	1.32	0.28	none	0.45	0.69
ω_0[$Pd(CO)_2$], cm^{-1}	2085	2010		1944	2029[b]
	2154	2052		1973	2059[b]
E_b[Rh(CO)→Rh+CO], eV	1.94	2.74	2.61	1.18	1.03
ω_0[Rh(CO)], cm^{-1}	2008	1999	1946	1930	2062
E_b[$Rh(CO)_2$→Rh(CO)+CO], eV	1.47	0.61	0.71	1.97	2.24
ω_0[$Rh(CO)_2$], cm^{-1}	2034	1949	1911	1881	
	2120	2017	1979	1931	
E_b[$Rh(CO)_3$→$Rh(CO)_2$+CO], eV	1.11	1.00		1.07	
ω_0[$Rh(CO)_3$], cm^{-1}	2043	1966		1896	
	2049	1969		1901	
	2107	2026		1953	

[a] The vibrational frequencies are scaled by a factor 0.977. [b] From ref 8.

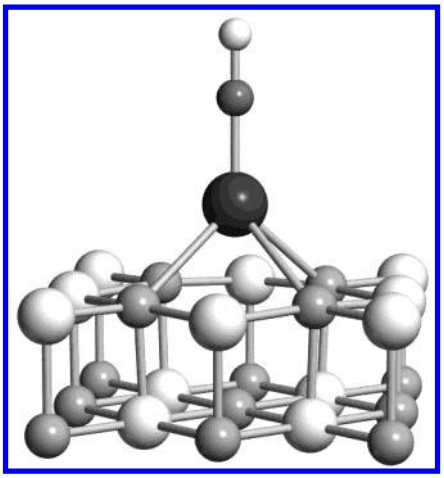

Figure 6. Structure used for the calculation of the properties of a M−CO complex adsorbed on the MgO (100) terrace or on an oxygen vacancy (F center) (shown in the figure). A full geometry optimization leads in some cases to CO molecules tilted from the surface normal; see text.

trapping site (an F center or a step) and bind it to a terrace O_{5c} anion (Table 3). These energy differences are not barriers for diffusion but represent lower bounds to the energy required to move an atom between two sites. While Pd can be relatively easily detrapped from a step site, Rh is more strongly bound (Table 3). On the other hand, similarly large energies are required to move Rh and Pd once they are bound to F centers. The effect of CO dosing and the consequent formation of M(CO) or $M(CO)_2$ complexes can change this picture and lead to a different mobility as the temperature is raised (Table 3). The Pd(CO) complexes seem to be more mobile than the corresponding Rh(CO) ones. In particular we notice that the barrier to move the Rh(CO) complex from a surface O_{5c} anion to the nearest one, going through the bridge position, requires almost 1 eV. Similar energy is needed to displace Rh(CO) from a step to an O_{5c} site. For Pd(CO), the corresponding energies are about 0.3 eV lower.

We consider now the properties of CO adsorbed to the deposited metal atoms. In these calculations we assumed that the CO molecule is bound with its axis normal to the surface plane, and the geometry optimization has been done in C_{4v} symmetry (Figure 6). Removing all geometrical constraints, we found that in some cases the best geometry is with the CO molecule tilted with respect to the surface normal.[28] The tilt angle depends on the metal and adsorption site. However, the energy for the tilting is very small, and the adsorption properties (binding energy and CO vibration) are similar for bent and normal orientations.[28] We first consider Ag. At the B3LYP level the Ag(CO) gas-phase complex is unbound. The deposition of the Ag atom on the MgO surface does not change the situation, and we do not observe formation of the O_{5c}/Ag(CO) complex (Table 4). Very weak Ag−CO bonds (less than 0.2 eV) are found when Ag is stabilized at F_{5c} or F_{5c}^+ centers or at steps, but this bonding could arise entirely from the BSSE. These results tend to exclude that Ag(CO) complexes form on the surface. The bonding of Ag with the MgO surface is mainly due to polarization effects, without changes in the Ag atom electronic structure.[29] The Ag atom maintains the 5s electron in the valence, thus preventing the CO molecule from coming close enough to give rise to a sufficient $4d_{\pi}$–$2\pi^*$ interaction. In this respect, it is not surprising that no bonding is found for either the gas-phase or the supported Ag−CO complexes. However, the formation of van der Waals complexes cannot be excluded at this level since DFT is not appropriate to describe dispersive forces.

Rh and Pd adsorbed on MgO have $4d^9$ and $4d^{10}$ electronic configurations, respectively, and form strong bonds with the CO molecule. The results show that, going from the free Rh(CO) or Pd(CO) molecules to the surface complexes, the metal−CO bond strength changes depending on the adsorption site. On terrace oxygen anions there is an increase in the metal−CO binding (from 1.80 to 2.34 eV for Pd and from 1.94 to 2.74 eV for Rh (Table 4)). The effect is similar when the metal is adsorbed at a step. The increase in metal−CO bond strength on the surface is justified by the enhanced back-donation ability of the metal atom (charge flows from the oxide anion to the metal and from this to CO). The situation is reversed when the metal atom is stabilized at an F center: here, the formation of a strong metal−oxide bond (Table 2) results in a weakening of the metal−CO interaction. For Pd this is more pronounced and the bonding with CO goes from 1.80 eV in the gas-phase to 0.6−0.8 eV on F_{5c} centers (Table 4). For Rh the change is smaller, from 1.94 eV in the free molecule to 1−1.2 eV on F_{5c} centers (Table 4). A significant difference between Pd and Rh, which is important for explaining the observed behavior, is the tendency of Rh to bind more CO molecules. $Rh(CO)_2$ and $Rh(CO)_3$ complexes form both on oxide anions and F centers, while $Pd(CO)_2$ is not very stable, and $Pd(CO)_3$ does not form at all.

4. Discussion

4.1. Ag/MgO. We have seen above the theory to predict that Ag(CO) complexes do not form on MgO. This opens the

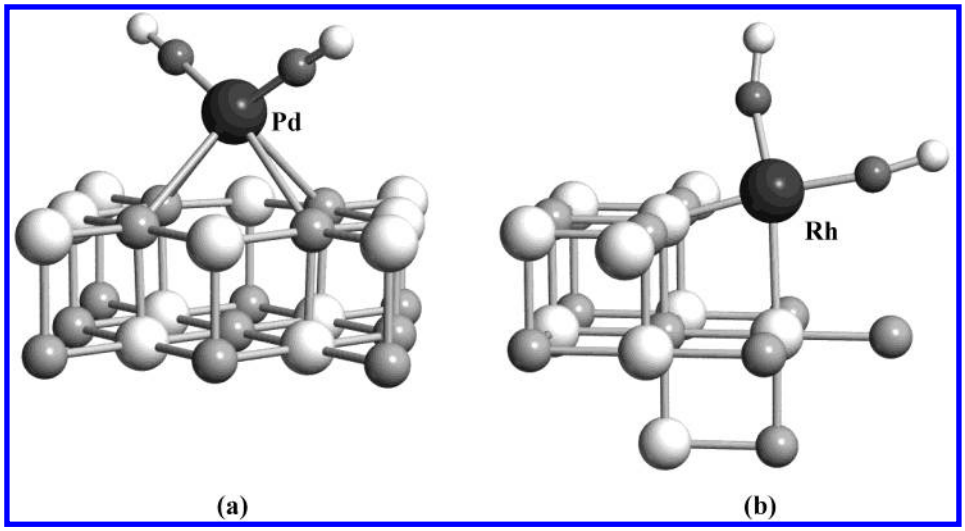

Figure 7. Optimal geometry of $M(CO)_2$ complexes adsorbed on the MgO surface. (a) $Pd(CO)_2$ complex formed at an oxygen vacancy (F center); (b) $Rh(CO)_2$ complex formed at a step.

question about the interpretation of the TD spectra (Figure 1), which show a small contribution to the CO desorption from the metal in the range of 130−200 K. A possible explanation is that the CO molecules are bound only at Mg^{2+} surface cations and that the preadsorbed Ag atoms have an indirect effect, which slightly reinforces the CO−MgO bond. This is further supported by the very similar vibrational frequencies measured for CO adsorbed on the clean MgO film and on the film after Ag deposition. The only change is a very small red-shift (8 cm^{-1}, Figure 2) and a small enhancement of the low-frequency band. The Ag atoms could slightly modify the surface potential (through small charge-transfer or polarization effects at the interface) or, less probably, provide a special adsorption site where the CO molecule interacts simultaneously with the surface cations and with a vicinal Ag atom. On these sites one could form a sort of van der Waals complex where the CO adsorption properties are only slightly perturbed compared to the bare MgO surface.

4.2. Pd/MgO. The TDS spectra show two CO desorption peaks at 230 and 370 K, corresponding to Pd−CO binding energies of 0.6 and 1.0 eV, respectively (Figure 1). The changes in the TDS spectra going from clean MgO to Pd_1/MgO clearly indicate a direct role of Pd in the CO adsorption. The second high-energy peak is associated with a strong change in the CO ω_e, which is typical of bridge-bonded CO, indicating the formation of dimers or larger Pd aggregates. In a previous study[8] we have shown that a Pd−CO binding of 0.6 eV is incompatible with Pd atoms sitting on O_{5c} sites (see also Table 4). In fact, a O_{5c}/Pd(CO) complex is characterized by a Pd−CO bond strength of 2.34 eV; if we assume that the Pd atom is stabilized at step sites, we still have a Pd−CO binding of 2.32 eV, four times larger than in the experiment. On the other hand, if we assume the Pd to be bound on an F_{5c} or F_{5c}^+ center, the computed Pd−CO bond strength is of 0.63 and 0.82 eV (Table 4), respectively, two values consistent with the TD spectra. The presence of two vibrational frequencies between 90 and 250 K, however, indicates that two CO molecules are adsorbed on the Pd atoms, a fact which considerably complicates the picture. We consider first the arguments in favor of the original interpretation (Pd atoms stabilized at F centers already at low temperature).[8] On a terrace F_{5c} or F_{5c}^+ center the $Pd(CO)_2$ complex (Figure 7a) is stable although the second CO molecule is less strongly bound than the first one (E_b for the second CO is 0.45 eV for F_{5c} and 0.69 eV for F_{5c}^+; Table 4). Since the CO dosage is sufficiently large to saturate all Pd atoms with two CO molecules, $Pd(CO)_2$ complexes can form at F or F^+ centers. This implies that the Pd atoms arriving from the gas phase have sufficient mobility to diffuse and become stabilized at preexisting point defects such as F centers. Our results tend to exclude that the species diffusing to the F centers are Pd(CO) or $Pd(CO)_2$ complexes. In fact, the diffusion of a Pd(CO) complex from O_{5c} to a F_{5c} center results in an energy gain of 0.84 eV (Table 3). This energy exceeds the bonding of CO to Pd/F_{5c} (0.63 eV, Table 4). In other words, the energy released when Pd(CO) is stabilized at a F_{5c} center could be sufficient to desorb the CO molecule (the same argument applies to $Pd(CO)_2$). Thus, it is more likely that the Pd atoms are already trapped at the F centers when the sample is exposed to CO and that F_{5c}/$Pd(CO)_2$ or F_{5c}^+/$Pd(CO)_2$ complexes form for T < 250 K. By raising the temperature, the first CO desorption occurs at relatively low energy (0.45 eV for F_{5c} and 0.69 eV for F_{5c}^+ centers); this leaves on the surface a F_{5c} (or F_{5c}^+)/Pd(CO) complex where the CO molecule is moderately bound, 0.63 eV on F_{5c} and 0.82 eV on F_{5c}^+ centers (Table 4). Therefore, for T > 250 K no CO molecules are present on Pd atoms bound at F centers.

The calculations for the CO vibrational frequencies show that on an F center there are two bands at 1944 and 1973 cm^{-1} and that by desorbing one CO the frequency shifts to 2013 cm^{-1} (Table 4); on F_{5c}^+ the frequencies are 2029 and 2059 cm^{-1} for $Pd(CO)_2$[8] and 2091 cm^{-1} for Pd(CO). Note that the normal component of the total dynamic dipole of the asymmetric stretch mode of the $Pd(CO)_2$ complex is zero and can therefore not be observed in our experiment. The values for the F_{5c} centers are considerably smaller than the experimental ones. This is either due to the use of PC fields, or an overestimation of the charge transfer from the F center to Pd, or to a combination of these effects. To explain the high-energy peak in the TDS, attributed to Pd aggregates, we must assume that the residual Pd atoms or Pd(CO) species bound at terraces or steps diffuse until they interact with Pd atoms bound at F_{5c} sites where the nucleation of small clusters occurs.

Based on the starting hypothesis that Pd atoms do not diffuse and that $Pd(CO)_2$ complexes form on O_{5c} sites, there is another, completely different interpretation of the results. The binding energies of the two CO molecules in O_{5c}/$Pd(CO)_2$ differ by an order of magnitude: while the first CO molecule binds by 2.34 eV, the second is only weakly bond, by 0.28 eV. This value is overestimated by the BSSE and the real binding could be even

weaker. Notice that on a step $Pd(CO)_2$ does not form (Table 4). Still, assuming that our CO binding energies are underestimated by 0.5 eV or more, one could propose that at $T = 230$ K one observes the desorption of the second CO molecule from $O_{5c}/Pd(CO)_2$ (0.6 eV in the experiment, <0.28 eV in the calculations). This leaves on the surface $O_{5c}/Pd(CO)$ complexes where CO is so strongly bound (2.34 eV) that the Pd(CO) complex diffuses without dissociating until it becomes trapped at an F center, forming $F_{5c}/Pd(CO)$ and, at higher T, larger aggregates by condensation with another Pd(CO) unit. In favor of this hypothesis are the computed vibrational frequencies of the $O_{5c}/Pd(CO)$ and $O_{5c}/Pd(CO)_2$ complexes (Table 4), although the uncertainties in these quantities are such that a firm assignment is not possible. Against this mechanism are two considerations: (a) the computed dissociation of the first CO is much lower than the measured one, and (b) as we mentioned above, if Pd(CO) diffuses from an O_{5c} site to an F center this could results in the spontaneous release of CO because of the heat of adsorption of Pd(CO) to a F_{5c} center. The hypothesis that the Pd atoms are bound at O_{5c} sites is also in complete disagreement with another series of experiments and related calculations.[10,30] Pd atoms deposited on MgO have been exposed to acetylene, and the reaction of the hydrocarbon molecule to form benzene rings has been studied in great detail. The results have shown that the hypothesis that the Pd atoms sit on the oxygen sites of the MgO surface is completely incompatible with the temperature at which the reaction occurs (300 K). On the contrary, assuming that the Pd atoms are bound at F or F^+ centers, it has been possible to explain a large number of features, including the reaction mechanism.[31] Therefore, the original interpretation that the Pd atoms are stabilized at F centers already at low temperature seems more realistic.

4.3. Rh/MgO. As for Pd two CO desorption peaks have been observed in the TD spectra (Figure 1), one at 180 K (corresponding to a Rh−CO binding of 0.5 eV) and one at 390 K (corresponding to a desorption barrier of 1.1 eV). The second feature is more pronounced, and we explained above that the high-energy binding site is populated already at low temperature. The IR data show unambiguously that there is no formation of Rh aggregates, at variance with Pd. Thus, Rh is stabilized at two different sites, site A stable up to 250 K and site B which is populated up to $T = 450$ K (at this temperature all CO molecules have desorbed; see the IR spectra of Figure 4). The calculations show that significant differences between Rh and Pd are (a) the tendency of Rh to bind two or even three CO molecules more strongly than Pd and (b) a smaller mobility of Rh(CO) complexes on the surface. On a O_{5c} site a Rh atom binds a CO molecule with $E_b = 2.74$ eV (Table 4); the addition of a second CO molecule leads to an additional energy gain of 0.61 eV (it is of only 0.28 eV on Pd); the third CO molecule is bound by 1.00 eV (Pd does not bind a third CO molecule). The energy required to desorb one or two CO molecules from $O_{5c}/Rh(CO)_2$ to $O_{5c}/Rh(CO)_3$, 0.6−1.0 eV, is close to that deduced from the TD spectra, 0.5 eV, in particular considering the BSSE correction; in this respect the hypothesis that $O_{5c}/Rh(CO)_2$ or even $O_{5c}/Rh(CO)_3$ complexes form at low temperature is supported by the computed energy values. What is less satisfactory in this context is the analysis of the computed vibrational frequencies. The experimental values for ^{13}CO are 2010 and 2040 cm^{-1}. Assuming an isotope effect of about 40 cm^{-1} leads to ^{12}CO frequencies of ≈2050 and ≈2080 cm^{-1}. Matrix isolated Rh(CO) complexes show a CO ω_e of 2008−2020 cm^{-1} (Table 4). Thus, on the MgO surface there is a blue shift of at least 40−60 cm^{-1}. Very similar vibrations have been measured for $Rh(CO)_2$ complexes on alumina by Yates and coworkers and,[32,33] more recently, on alumina thin films by Frank et al.[34,35] The shift with respect to matrix isolated Rh(CO) can have three origins: (1) the Rh atoms are oxidized on the surface and transform into Rh^I, thus reducing the Rh-to-CO back-donation; (2) two CO molecules are bound to the same metal so that the back-donation is reduced with consequent increase of the C−O frequency; (3) the CO−CO dipole coupling contributes to the blue shift, explaining also the double peak in the spectrum. Several attempts have been made to model sites where the Rh atom could be oxidized to Rh^I (including Mg vacancies, surface peroxo groups, etc.): none of the sites considered has provided a picture consistent with the other observations, such as, for instance, the CO desorption energy. On the basis of these results, we tend to exclude the presence of Rh^I atoms on the surface. This is also consistent with the general idea that the MgO surface presents several basic sites, like the oxygen anions, while there are no strong acid sites. The hypothesis that the reduced back-donation and the CO−CO coupling are the origins of the blue shift is therefore much more realistic. The calculations for the gas-phase $Rh(CO)_2$ complex (a linear molecule) give symmetric and antisymmetric stretches at 2121 and 2034 cm^{-1}, with a large blue shift with respect to Rh(CO) and a dipole coupling of ≈90 cm^{-1}. However, once deposited on the surface, the coupling becomes about 40 cm^{-1}, and the frequencies are found at 1949 and 2017 cm^{-1}, i.e., red-shifted with respect to gas-phase Rh(CO) (Table 4). As discussed above, a red-shift of 30−50 cm^{-1} is an artificial effect of the field created by the PC's. Even assuming this correction, our values seem to be underestimated compared to the observed ones. We did consider also the $O_{5c}/Rh(CO)_3$ complex, but the highest frequency is found at 2026 cm^{-1} (Table 4), still far from the ≈2080 cm^{-1} experimental value for ^{12}CO. Thus, with the assumption that the Rh atoms sit on surface O_{5c} anions we have a problem in explaining the relatively high frequencies observed. Possible reasons for this underestimate have been given above.

Assuming that the discrepancy has to be attributed to limitations in the calculations, we can conclude that the best candidate for site A where $Rh(CO)_x$ complexes form are the surface oxygen ions. In fact, the F centers, which are the most likely sites for Pd atoms, are less probable in the case of Rh. The reasoning is the following. On a F_{5c}/Rh complex the first CO molecule is bound by 1.18 eV [$F_{5c}/Rh(CO)$], the second by 1.97 eV [$F_{5c}/Rh(CO)_2$], and the third one by 1.07 eV [$F_{5c}/Rh(CO)_3$]. This shows the great stability of Rh carbonyl complexes on electron-rich centers such as the O vacancies. This seems to exclude the possibility that $Rh(CO)_2$ units form at low temperature on F_{5c} centers for two reasons: (1) the second CO molecule is too strongly bound (3 times more than the experimental estimate for the low-temperature peak in TDS); (2) the second CO is more strongly bound than the first one, so that the two molecules should desorb together, giving a single TDS peak. The idea that a $Rh(CO)_3$ complex forms on a F_{5c} center could explain the first peak in the TDS result (E_b for the third CO molecule is 1.07 eV, to be compared with the 0.5 eV value deduced from the spectra) but cannot explain the second peak. As usual, the vibrational frequencies of the $F_{5c}/Rh(CO)_2$ complex are too low (from 1881 to 1931 cm^{-1}) compared to the observed data. Still, it is possible that a fraction of the Rh atoms is stabilized at F centers already at low temperature and that $Rh(CO)_2$ forms on these sites. The shape of the IR band between 1900 and 2000 cm^{-1} for $T < 250$ K suggests in fact the presence of more Rh−carbonyl species on the surface.

On this basis, we propose that at low temperature Rh−carbonyl complexes form mostly on O sites (site A) and that a minority populates the F centers. What remains to be clarified is the type of O sites. Bridge-bonded terrace sites with the Rh atoms equidistant from two surface O_{5c} anions are not local minima, and the geometry optimization always gives the O_{5c} on-top site as the preferred one (see Table 3). The other possibility is a step (Figure 7b). In this site the Rh atom can bind simultaneously with an O_{4c} (step) and an O_{5c} (terrace) site. The binding of the isolated Rh atom to this site is close to 2 eV, i.e., about twice that for an O_{5c} terrace site (Table 2). CO binds to a Rh atom at a step with a binding energy of 2.61 eV [O_{4c}–O_{5c}/Rh(CO)], close to that found for Rh on O_{5c} sites (2.74 eV). The second CO molecule is bound by 0.71 eV, a value which is consistent with the first desorption peak in TDS. The vibrational frequencies for a step O_{4c}–O_{5c}/$Rh(CO)_2$ are somewhat smaller than for the terrace O_{5c}/$Rh(CO)_2$ case (Table 4). In this respect, terrace or step sites are equally probable candidates for site A. However, considering that the bonding of Rh to a step is stronger than on a terrace, it is more likely that the $Rh(CO)_x$ complexes form at these sites. Notice that Pd atoms adsorbed at steps do not bind a second CO molecule and are easily detrapped, a fact which could explain the different behavior of Rh and Pd.

To summarize this part, $Rh(CO)_2$ or $Rh(CO)_3$ complexes form at oxygen sites (most likely steps) for $T < 180$ K; at higher temperatures the complex loses CO and transforms into supported Rh(CO) units. The Rh−CO bonding is so strong (2.6−2.7 eV) that this unit diffuses on the surface without breaking apart until it becomes stabilized at strong trapping sites (site B). To identify this second site, we have to explain two features: at site B the Rh−CO dissociation requires about 1.1 eV; going from site A to site B there is a red shift of 50 cm^{-1} of ^{13}CO ω_e, from about 2000 cm^{-1} at $T = 300$ K to 1956 cm^{-1} at $T = 380$ K (Figure 4). In principle, site B could correspond to a step oxide anion and site A to a terrace oxide anion and the migration could involve these two sites. However, the fact that the Rh−CO binding at a step is 2.6 eV, while the experimental value is 1.1 eV rules out this as a possible explanation. Natural candidates for site B are the F centers. The CO dissociation in F_{5c}/Rh(CO), 1.18 eV, is quite consistent with this assumption. Notice that, at variance with Pd, the displacement of a Rh(CO) molecule from an O_{5c} to a F_{5c} site implies an energy gain of 0.83 eV (Table 3), while the Rh−CO bond at an F center is 1.18 eV (Table 4). Thus, spontaneous dissociation of CO is not expected for Rh going to site A (step) to site B (F center). Moving Rh(CO) from a step (site A) to a F_{5c} center (site B), the CO vibrational frequency is slightly redshifted (Table 4), consistent with the observation. For the F_{5c}/Rh(CO) complex, the CO ω_e is 1930 cm^{-1} and the experimental value 1956 cm^{-1}, consistent with the general underestimate of CO frequencies for supported metal−CO complexes. Finally, we notice that F_{5c}^+ centers can be ruled out as candidates for site B because on these sites the CO ω_e is blue-shifted with respect to site A, contrary to experiment.

5. Conclusions

In this work we have studied the properties of CO molecules adsorbed on metal atoms deposited on MgO thin films. In particular, the evolution of the system as a function of the temperature has been analyzed in detail. This provides a way to shed some light on the surface sites, which bind the metal atoms, on the role of point and extended defects as well as on the mechanisms of the diffusion of atoms or carbonyl complexes on the surface. The combined analysis of the TD and FTIR spectra and of first principles calculations allows us to formulate or to rule out some working hypothesis.

Deposition of Ag atoms represents the simplest case due to the low adhesion of Ag to MgO and to the absence of reactivity of the deposited Ag atoms. The calculations exclude the formation of stable Ag−CO complexes at any of the surface sites considered (regular sites or point defects). This leads us to interpret the small changes in the TD and FTIR spectra before and after Ag deposition either as an indirect effect, mainly due to local changes in the surface potential induced by the presence of the metal atoms, or as due to the formation of van der Waals complexes.

Deposition of Pd followed by exposure to CO has been considered in a previous work[8] and is analyzed here because of some new data but also to provide a consistent comparison with Rh. At low temperature ($T < 300$ K) we observe the formation of $Pd(CO)_2$ species, while at higher temperatures there is formation of Pd aggregates. Most likely, the Pd atoms possess a sufficient mobility on the surface to diffuse and become stabilized at strong trapping sites before CO exposure. The best candidates for trapping the Pd atoms are the oxygen vacancies (F centers). By exposure to CO, Pd(CO) and $Pd(CO)_2$ complexes form on F centers. The CO molecules are desorbed from these sites at low temperature ($T = 230$ K; $E_b = 0.6$ eV). By further raising the temperature, residual Pd atoms or Pd(CO) units diffuse on the surface until they aggregate to form larger particles.

Another hypothesis, which seems less likely on the basis of our theoretical results, is that the Pd atoms do not diffuse on the surface but are bound at oxide sites at the terraces of MgO. Here, $Pd(CO)_2$ complexes form (notice that this is not possible if the Pd atoms are bound to steps); the first CO desorption at 230 K leaves on the surface a Pd(CO) unit, which easily diffuses until it becomes trapped, at higher temperature, at an F center. In this model the F centers are nucleation sites for small Pd or $Pd_x(CO)_y$ clusters. This second possibility presents some internal inconsistencies and contradicts previous results on the mechanism of acetylene cyclotrimerization on Pd_1/MgO, which show the important role of F centers in the activation of the Pd atoms already at 90 K.[10]

Rh atoms can diffuse on the surface, but they bind quite strongly with step sites (more than Pd). Only a small fraction of Rh atoms populates the F centers at low temperature. The exposure to CO leads to the formation of relatively stable $Rh(CO)_2$ complexes at steps, at variance with Pd. The first CO desorption leaves on the surface rather mobile Rh(CO) units, which diffuse until they become trapped at F centers. A further increase in the temperature leads to a second desorption of CO from Rh atoms at F centers.

The results presented, and the tentative explanations provided, clearly indicate that the deposition of metal atoms on the MgO films is followed by complex diffusion mechanisms, which depend quite strongly on the nature of the metal−MgO bond. The use of CO as a probe molecule provides invaluable information for identifying the metal adsorption sites but also contributes to complicating the diffusion mechanisms as new M−CO species, quite strongly bound in the case of Rh and Pd, can become mobile on the surface and compete with the mobility of the individual metal atoms.

Acknowledgment. K.J. thanks the Humboldt Foundation for financial support, S.A. thanks the Swiss National Science Foundation and the Humboldt Foundation for financial support,

and A.S.W. acknowledges support of the Graduiertenkolleg "Molekulare Organisation und Dynamik an Grenz- und Oberflächen". The experimental work was supported by the Deutsche Forschungsgemeinschaft. L.G. and G.P. thank the Italian INFM for financial support through the PRA-Project ISADORA and computer time allocated at the CINECA computing center.

References and Notes

(1) Freund, H. J. *Surf. Sci.* **2002**, *500* 271.
(2) Binnis, C. *Surf. Sci. Rep.* **2001**, *44*, 1.
(3) Guzman, J.; Gates, B. C. *Nanoletters* **2001**, *1*, 689.
(4) *Chemisorption and Reactivity on Supported Clusters and Thin Films*; Lambert, R. M., Pacchioni, G., Eds.; NATO ASI Series E, Vol. 331; Kluwer: Dordrecht, The Netherlands, 1997.
(5) Heiz, U.; Vanolli, F.; Trento, L.; Schneider, W.-D. *Rev. Sci. Instrum.* **1997**, *68*, 1986. From NO desorption experiments a minimal defect density of 1% ML was estimated (Heiz, U.; Schneider, W.-D. *J. Phys. D: Appl. Phys.* **2000**, *33*, R85−R102). The absence of a vibrational band typical for bridge-bonded CO suggests, however, that the total defect density is considerably higher.
(6) Abbet, S.; Judai, K.; Klinger, L.; Heiz, U. *Pure Appl. Chem.* **2002**, *74*, 1527.
(7) Cheng, H. P.; Landman, U. *J. Phys. Chem. A* **1999**, *103*, 9573.
(8) Abbet, S.; Riedo, E.; Brune, H.; Heiz, U.; Ferrari, A. M.; Giordano, L.; Pacchioni, G. *J. Am. Chem. Soc.* **2001**, *123* 6172.
(9) Häkkinen, H.; Abbet, S.; Sanchez, A.; Heiz, U.; Landman, U. *Angew. Chem.*, in press.
(10) Abbet, S.; Sanchez, A.; Heiz, U.; Schneider, W. D.; Ferrari, A. M.; Pacchioni, G.; Rösch, N. *J. Am. Chem. Soc.* **2000**, *122*, 3453.
(11) Sanchez, A.; Abbbet, S.; Heiz, U.; Schneider, W.-D.; Häkkinen, H.; Barnett, R. N.; Landman, U. *J. Phys. Chem. A* **1999**, *103*.
(12) Wu, M. C.; Corneille, J. S.; Estrada, C. A.; He, J.-W.; Goodman D. W. *Chem. Phys. Lett.* **1991**, *182*, 472.
(13) Schaffner, M.-H.; Patthey, F.; Schneider, W.-D. *Surf. Sci.* **1998**, *417*, 159.
(14) *Cluster Models for Surface and Bulk Phenomena*; Pacchioni, G., Bagus, P. S., Parmigiani, F., Eds.; NATO ASI Series B, Vol. 283; Plenum Press: New York, 1992.
(15) Becke, A. D. *Phys. Rev. A* **1998**, *38*, 3098.
(16) Lee, C.; Yang, W.; Parr, R. G. *Phys. Rev. B* **1988**, *37*, 785.
(17) Ferrari, A. M.; Pacchioni, G. *Int. J. Quantum Chem.* **1996**, *58*, 241.
(18) Pacchioni, G. *Surf. Rev. Lett.* **2000**, *7*, 277.
(19) Ditchfield, R.; Hehre, W.; Pople, J. A. *J. Chem. Phys.* **1971**, *54*, 724.
(20) Ferrari, A. M.; Soave, R.; D'Ercole, A.; Pisani, C.; Giamello, E.; Pacchioni, G. *Surf. Sci.* **2001**, *83*, 479.
(21) Hay, P. J.; Wadt, W. R. *J. Chem. Phys.* **1985**, *82*, 299.
(22) Boys, S.; Bernardi, F. *Mol. Phys.* **1970**, *19*, 553.
(23) Herzberg, G. *Molecular Spectra and Molecular Structure*, Vol. 1; Van Nostrand: Princeton, NJ, 1950).
(24) Pelmenshikov, A. G.; Morosi, G.; Gamba, A.; Coluccia, A. *J. Phys. Chem.* **1995**, *99*, 15018.
(25) Frisch, M. J.; et al. *Gaussian98*; Gaussian, Inc.: Pittsburgh, PA, 1998.
(26) Abbet, S.; Heiz, U.; Häkkinen, H.; Landman, U. *Phys. Rev. Lett.* **2001**, *86*, 5950.
(27) Wovchko, E. A.; Yates, J. T., Jr. *Langmuir* **1999**, *15*, 3506.
(28) Giordano, L.; Ferrari, A. M.; Del Vitto, A.; Pacchioni, G. *Surf. Sci.* **2003**, *540*(1), 63.
(29) Yudanov, I.; Pacchioni, G.; Neyman, K.; Rösch, N. *J. Phys. Chem.* **1997**, *101*, 2786.
(30) Ferrari, A. M.; Giordano, L.; Rösch, N.; Heiz, U.; Abbet, S.; Sanchez, A.; Pacchioni, G. *J. Phys. Chem. B* **2000**, *104*, 10612.
(31) Ferrari, A. M.; Giordano, L.; Pacchioni, G.; Abbet, S.; Heiz, U. *J. Phys. Chem. B* **2002**, *106*, 3173.
(32) Wovchko, E.; Yates, J. T. *Langmuir* **1999**, *15*, 3506.
(33) Wovchko, E.; Yates, J. T. *J. Am. Chem. Soc.* **1995**, *117*, 12557.
(34) Frank, M.; Bäumer, M. *Phys. Chem. Chem. Phys.* **2000**, *2*, 3723.
(35) Frank, M.; Bäumer, M.; Kühnemuth, R.; Freund, H. J. *J. Phys. Chem. B* **2001**, *105*, 8569.